张兆鑫, 曹宁宁, 李林记, 等. 原位吸附技术修复六价铬污染土壤[J]. 岩矿测试, 2024, 43(2): 302−314. DOI: 10.15898/j.ykcs.202307090090.
ZHANG Zhaoxin, CAO Ningning, LI Linji, et al. *In situ* Adsorption Technology for Remediation of Cr(Ⅵ) Contaminated Soil[J]. Rock and Mineral Analysis, 2024, 43(2): 302−314. DOI: 10.15898/j.ykcs.202307090090.

原位吸附技术修复六价铬污染土壤

张兆鑫[1,2,3]，曹宁宁[1]，李林记[1,2]，刘素青[1]，李佳昊[1]，曹翠[1]，李和平[1]，张凯[1]，石勇丽[1,2,3*]
(1. 河南省地质研究院 (地质实验测试所)，河南 郑州 450018；
2. 自然资源部黄河流域中下游水土资源保护与修复重点实验室，河南 郑州 450052；
3. 河南省自然资源科技创新中心 (水土生态修复治理研究)，河南 郑州 450052)

摘要：常见六价铬 Cr(Ⅵ) 污染场地修复技术如客土法、还原法、固化法、生物法等存在成本高、效率低及 Cr(Ⅵ) 被二次氧化等缺点。理想修复技术应能快速、低成本地将铬元素 (Cr) 从土壤中彻底去除。本文将聚吡咯 (PPy) 通过原位聚合的方式负载在凹凸棒土 (ATP) 表面，制备了以 PPy 为“壳”和以 ATP 为“核”的 ATP/PPy 复合材料，ATP/PPy 对 Cr(Ⅵ) 的最大吸附容量为 185.19mg/g，吸附机理包括静电引力、螯合、还原与离子交换等。将 ATP/PPy 嵌入土壤中，利用 Cr(Ⅵ) 在土壤中的纵向迁移及横向浓度差渗透，可实现对土壤中 Cr(Ⅵ) 的原位吸附。实验考察了模拟降雨量、土壤 pH、土壤容重、土壤有机质含量等因素对土壤中 Cr(Ⅵ) 去除效率的影响。结果表明，当供试土壤中 Cr(Ⅵ) 浓度为 30mg/kg，模拟降雨量为 6mL/天，土壤有机质含量为 7.6g/kg，土壤容重为 1.22g/cm^3，土壤 pH 为 5.86 时，第 35 天时土壤滤液中 Cr(Ⅵ) 去除率为 58.51%，土壤中 Cr(Ⅵ) 含量降低至 2.97mg/kg，低于《土壤环境质量建设用地土壤污染风险管控标准 (试行)》(GB36600—2018) 中的建设用地第二类用地筛选值 5.7mg/kg。该技术具有操作简单、经济环保、效率高、去除彻底等优势，可为污染场地的高效低成本治理提供新思路及技术支撑。

关键词：凹凸棒土；聚吡咯；土壤修复；六价铬；原位吸附

要点：

(1) 制备了对 Cr(Ⅵ) 有强吸附亲和力的 ATP/PPy 复合材料，ATP/PPy 能有效地去除水溶液和土壤中的 Cr(Ⅵ)，吸附机理包括静电引力、螯合、还原与离子交换。

(2)ATP/PPy 对 Cr(Ⅵ) 的吸附遵循伪二级动力学模型，说明吸附过程主要是化学吸附。ATP/PPy 对 Cr(Ⅵ) 的吸附遵循 Langmuir 等温模型，说明吸附过程是单层吸附，最大吸附量为 185.19mg/g。

(3)ATP/PPy 通过原位吸附技术修复 Cr(Ⅵ) 污染土壤实验表明，当供试土壤中 Cr(Ⅵ) 浓度为 30mg/kg，模拟降雨量为 6mL/天，土壤有机质含量为 7.6g/kg，土壤容重为 1.22g/cm^3，土壤 pH 为 5.86，第 35 天时土壤滤液中 Cr(Ⅵ) 去除率为 58.51%，土壤中 Cr(Ⅵ) 含量降低至 2.97mg/kg。

中图分类号：X53 **文献标识码：**A

铬 (Cr) 被广泛应用于工业和农业活动中，被国际社会列为最具有竞争力的 8 种资源性原材料产品之一[1-3]。随着工业的发展，大量 Cr 伴随着废水、废渣排放至环境中，留下了大量 Cr 污染场地[4-6]。

收稿日期：2023−07−09；**修回日期：**2023−12−01；**接受日期：**2024−02−05
基金项目：河南省科技攻关项目“基于六价铬污染场地原位修复材料开发研究”(212102310081)；河南省科技攻关项目“基于水中新兴污染物精准识别检测及高效去除技术研发”(232102320125)；河南省煤田地质局科研项目“黄河流域中下游耕地土壤重金属污染修复技术研发”；河南省地质研究院揭榜挂帅项目 (2023-906-XM012-KT02，2023-906-XM015-KT05)
第一作者：张兆鑫，硕士，工程师，主要从事水土生态修复治理工作。E-mail：hnmtzj@163.com。
通信作者：石勇丽，硕士，高级工程师，主要从事环境修复工作。E-mail：422081518@qq.com。

土壤中 Cr 主要以三价铬 Cr(Ⅲ) 和 Cr(Ⅵ) 的价态存在, 由于土壤主要带负电荷, Cr(Ⅲ) 在土壤中容易被土壤胶体吸附或形成沉淀, 活性较低, 对生物毒害作用较小。而 Cr(Ⅵ) 与土壤胶体吸附作用较弱、迁移性强、活性高, 易随着食物链的富集进入人体。Cr(Ⅵ) 进入人体后, 其阴离子化合物 (CrO_4^{2-}) 的化学结构与细胞内液中的 SO_4^{2-}和 HPO_4^{2-}相似, 可以很容易地通过细胞膜中蛋白通道进入细胞内部, 与细胞内抗坏血酸等还原性物质发生反应, 进而破坏细胞核内 DNA 并引起疾病, 如肺癌、出生缺陷和生殖能力下降等[7]。由于 Cr(Ⅵ) 的巨大危害性, Cr(Ⅵ) 及其化合物被美国环境保护署 (EPA) 列为 17 种高度危险的毒性物质之一[8-10], 因此对 Cr(Ⅵ) 污染场地的修复治理研究受到了各国环境工作者广泛关注。

据报道, 美国污染场地中 11% 为 Cr 污染, 日本污染场地中 14% 为 Cr(Ⅵ) 污染[11], 中国耕地污染土壤中 5% 以上为 Cr 污染[12]。近年来, 研究者开发了各种原位和异位修复技术, 以容纳、清理或恢复 Cr 污染土壤, 如客土法、土壤冲洗、电动修复、化学还原和植物修复等[13-16]。这些 Cr 污染土壤修复技术工作机制不同, 并显示出特定的应用优势和局限性。另外, 由于土壤的理化性质、质地、污染情况等不同, 这些修复技术在现场实践中的有效性和成本差异很大。如客土法与土壤冲洗技术成本高, 对周边环境扰动较大, 仅适用于小范围与高浓度的 Cr(Ⅵ) 污染场地; 化学还原是常见的 Cr(Ⅵ) 污染场地修复方式, 但是被还原的 Cr(Ⅲ) 存在着二次氧化为 Cr(Ⅵ) 的风险; 电动修复能耗高, 实际场地修复效果不理想; 植物修复效率低, 周期长。基于绿色及可持续发展理念, 开发经济高效且对环境友好的 Cr(Ⅵ) 污染场地修复新技术、新方法及新材料是当前迫切需要解决的关键问题。

吸附修复技术由于绿色环保、几乎对环境不造成伤害, 能够有效地将 Cr 元素从土壤中去除, 是一种理想修复技术[17-19]。但由于吸附材料从土壤中回收困难, 且土壤中干扰离子较多, 对吸附材料的吸附特异性要求较高, 目前尚没有应用于土壤 Cr(Ⅵ) 污染修复治理中。基于此, 本文制备了对 Cr(Ⅵ) 具有高特异性及高亲和力的 ATP/PPy 吸附材料, 该材料可通过静电引力、螯合、还原与离子交换等方式去除 Cr(Ⅵ) 离子。将该材料通过课题组前期研发的吸附板技术 (CN114042745B) 嵌入土壤中, 通过 Cr(Ⅵ) 在土壤中的纵向迁移及浓度差渗透, 实现对土壤中 Cr(Ⅵ) 的原位吸附, 待吸附饱和后取出可完成对 ATP/PPy 回收及再生。使用《土壤和沉积物中 Cr(Ⅵ) 的测定 碱溶液提取-火焰原子吸收分光光度法》(HJ 1082—2019) 测定修复前后土壤中 Cr(Ⅵ) 含量, 分别考察了降雨量、土壤 pH、土壤容重和土壤有机质含量 4 种因素对 ATP/PPy 去除土壤中 Cr(Ⅵ) 效果的影响, 以了解该技术对 Cr(Ⅵ) 污染土壤修复的可行性, 为后续 Cr(Ⅵ) 污染场地修复提供理论依据和技术支撑。

1　实验部分

1.1　仪器与主要试剂

UV-2600 型紫外可见光谱仪 (日本岛津公司); PinAAcle900T 型石墨炉火焰原子吸收分光光度计 (美国 PerkinElmer 公司); ME-204E 型分析天平 (Mettler Toled 公司); 水浴恒温振荡器 (北京国环高科自动化技术研究院); Nicolet6700 型傅立叶变换红外光谱仪 (FTIR, 美国 ThermoFisher 公司); SU8010 型场发射扫描电子显微镜 (SEM, 日立高新技术有限公司); K-ALPHA 型 X 射线光电子能谱仪 (XPS, 美国 ThermoFisher 公司)。

凹凸棒土 (ATP, 江苏盱眙鑫源科技有限公司), 吡咯 (Py, 分析纯, 阿拉丁化学试剂有限公司)。盐酸、氢氧化钠及无水氯化铁 (分析纯, 国药化学试剂有限公司), 重铬酸钾 (分析纯, 国药化学试剂有限公司), 去离子水 (电导率＞18.0MΩ•cm)。

1.2　吸附材料制备

将 1g 凹凸棒土分散在 100mL 蒸馏水中, 加入 5mL 浓盐酸搅拌 2h, 然后滴加 1mL 吡咯单体溶液继续搅拌 4h, 接着加入 1mol/L 氯化铁溶液 10mL, 搅拌 0.5h, 在 4℃ 冰箱中静置 24h(图 1)。最后过滤沉淀, 用蒸馏水和乙醇洗涤至滤液无色, 在 60℃ 温度下干燥 4h, 研磨粉碎备用。

1.3　ATP/PPy 吸附性能实验

ATP/PPy 吸附性能实验在水溶液中进行, 使用稀盐酸调节水溶液 pH 值为 2.43, 然后加入一定量的重铬酸钾溶液, 配制成不同浓度的 Cr(Ⅵ) 溶液。所有吸附实验均是将 10mg 的 ATP/PPy 加入 30mL 的 Cr(Ⅵ) 溶液中完成, 温度控制为 25℃, 转速为 200r/min。吸附完成后使用 0.45μm 聚丙烯过滤器从溶液中分离 ATP/PPy, 并测定滤液中 Cr(Ⅵ) 含量 (测定方法见 1.4 节)。ATP/PPy 吸附容量 (mg/g) 计算公式如下:

$$q_e = \frac{(C_0 - C_t)}{M} \times V$$

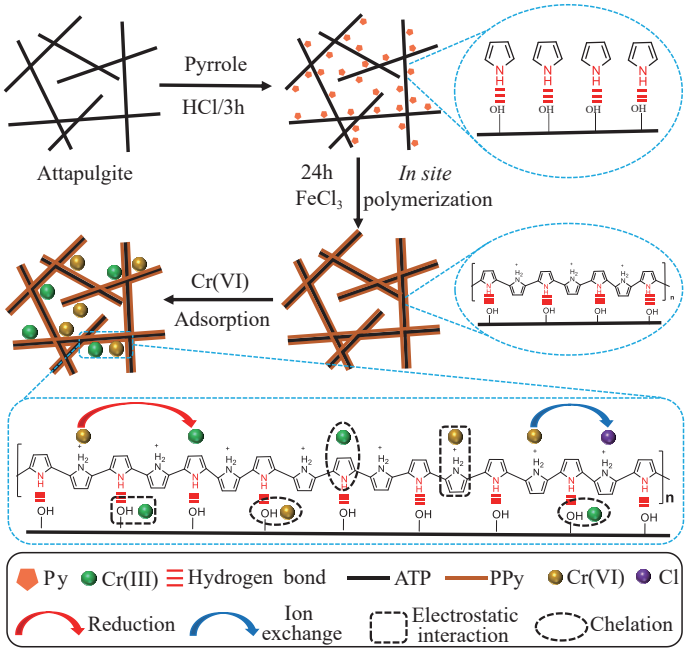

图1　ATP/PPy 吸附材料的制备及去除 Cr(Ⅵ) 机理示意图

Fig. 1　Schematic illustration of ATP/PPy synthesis and the mechanism for Cr(Ⅵ) removal.

式中: C_0 和 C_t 分别为溶液中 Cr(Ⅵ) 的初始和残留浓度 (mg/L), M 和 V 分别代表 ATP/PPy 质量 (g) 和 Cr(Ⅵ) 溶液体积 (L)。吸附动力学实验控制吸附时间分别为 10s、30s、2min、5min、30min、1h、2h、3h、4h、5h、6h, Cr(Ⅵ) 浓度为 50mg/L。吸附等温线实验控制 Cr(Ⅵ) 初始浓度分别为 40、60、80、100、120、150、170mg/L, 吸附时间为 32h。

1.4　土壤中 Cr(Ⅵ) 原位吸附去除实验

采集河南省郑州市某实验场地的三种类型土壤, 各类土壤理化性质分别为: 第一种土壤容重 1.08g/cm^3, pH 值 6.32, 有机质含量 2.53g/kg; 第二种土壤容重 1.22g/cm^3, pH 值 6.87, 有机质含量 1.36g/kg; 第三种土壤容重 1.41g/cm^3, pH 值 7.27, 有机质含量 1.14g/kg。采集的土壤通过添加盐酸和氢氧化钠溶液调节 pH, 通过添加有机肥 (发酵鸡粪) 调节土壤中有机质含量。

目前高浓度 Cr(Ⅵ) 污染土壤宜采用淋滤法修复治理, 而大面积、低浓度宜采用原位修复技术以节省修复成本, 因此本研究试验土壤采用中浓度 Cr(Ⅵ) 污染土壤 (30mg/kg)。通过向土壤中添加一定量重铬酸钾溶液, 并在室温中老化 30 天, 配制成 Cr(Ⅵ) 浓度为 30mg/kg 的试验土壤。取 20g 试验土壤加入到吸附柱中 (20mL 注射器, 内径为 1cm), 在土柱下面加入 10mg 的 ATP/PPy。采用单因素分析法, 考察降雨量、pH、土壤容重、土壤有机质含量等对 Cr(Ⅵ) 修复效果。每隔 5 天测定滤液体积及滤液中 Cr(Ⅵ) 浓度, 并计算滤液中 Cr(Ⅵ) 总质量。在第 35 天时测定土壤中 Cr(Ⅵ) 浓度, 另外设置不添加吸附材料组作为对照实验。依据《水质 六价铬的测定 二苯碳酰二肼分光光度法》(GB/T 7467—1987) 测定滤液中 Cr(Ⅵ) 浓度, 依据《土壤和沉积物中 Cr(Ⅵ) 的测定 碱溶液提取-火焰原子吸收分光光度法》(HJ 1082—2019) 测定土壤中 Cr(Ⅵ) 含量, 测试过程中标准曲线相关系数 R^2≥0.999。所有实验一式三份, 取平均值。

2　结果与讨论

2.1　ATP/PPy 吸附材料的表征

PPy 基吸附材料由于优异的还原性、离子交换性、静电引力及螯合性能, 常用于去除水中 Cr(Ⅵ)[20-22]。ATP 具有高比表面积及较多活性位点, 常用于功能材料载体[23-24]。基于此, 本研究将 PPy 以原位聚合方式负载在 ATP 表面, 形成了以 PPy 为“壳”和以 ATP 为“核”的核-壳复合结构 (图 1)。ATP 和 ATP/PPy 的形貌特征如图 2a 和图 2b 所示, 未经任何修饰的 ATP 为棒晶堆积形成的块状结构, ATP/PPy 为 PPy 微球包覆在 ATP 的表面, 同时在吸附 Cr(Ⅵ) 后, ATP/PPy 表面形貌几乎没有发生变化 (图 2c)。FTIR 光谱显示 (图 2d), ATP 在 3560cm^{-1} 和 3419cm^{-1} 处特征峰对应于矿物层和表面吸附水引

起的−OH 伸缩振动, 1665cm^{-1} 处特征峰对应于 H_2O 中−OH 的伸缩振动。此外, 1037cm^{-1} 和 791cm^{-1} 处特征峰分别归因于 Si−O−Si 伸缩振动和弯曲振动。PPy 在 1555cm^{-1} 处特征峰对应于吡咯环的 C=C 伸缩振动, 1160cm^{-1} 处特征峰对应 C−N 伸缩振动, 1030cm^{-1} 和 772cm^{-1} 处特征峰分别对应 C−H 面内伸缩振动峰和面外弯曲振动峰。FTIR 光谱清楚显示了 ATP/PPy 中具有PPy 的特征吸收峰, 表明 PPy 成功负载在 ATP 表面[25-26]。另外, ATP/PPy 吸附 Cr(Ⅵ) 后, ATP/PPy-Cr 红外谱带发生红移, 如 1565、1390、1210、1045 和 912cm^{-1}, 这是由于 ATP/PPy-Cr 中存在不同形态的 Cr, 导致 PPy 共轭结构被破坏及 PPy 电荷离域程度受到限制[22]。零点电位显示(图 2e), 由于 PPy 的引入, ATP/PPy 零点电位从 ATP 的 2.2 增加至 6.4, 零点电位的增强有利于 ATP/PPy 通过静电引力去除带负电的 Cr(Ⅵ)[27]。

2.2　ATP/PPy 对 Cr(Ⅵ) 的吸附性能

ATP/PPy 对 Cr(Ⅵ) 吸附动力学如图 3a 所示。实验表明 ATP/PPy 对 Cr(Ⅵ) 具有较快吸附速率, 在 30min 内可达到 95% 的平衡吸附量, 此后随着吸附时间增加, 吸附位点逐渐减少, 吸附过程趋于平衡。此外, 伪二级动力学模型完美拟合了 ATP/PPy 对 Cr(Ⅵ) 吸附数据, 相关系数 R^2>0.9999, 表明吸附过程主要是化学吸附[28-29]。为了研究 ATP/PPy 对 Cr(Ⅵ) 的最大吸附容量和吸附特性, 开展了吸附等温线研究, 如图 3b 所示。结果显示 ATP/PPy 对 Cr(Ⅵ) 的吸附容量随着 Cr(Ⅵ) 初始浓度增加而增加。Langmuir 模型很好地拟合 ATP/PPy 对 Cr(Ⅵ) 的吸附数据, 相关系数 R^2> 0.9996, 说明 ATP/PPy 对 Cr(Ⅵ) 吸附过程是单层吸附[30-31]。同时在 25℃ 时, ATP/PPy 对 Cr(Ⅵ) 最大吸附量为 185.19mg/g, 表明 ATP/PPy 对 Cr(Ⅵ) 有较大的吸附容量。

2.3　原位吸附技术对土壤 Cr(Ⅵ) 的修复效果

将 ATP/PPy 嵌入 Cr(Ⅵ) 污染土壤中, 利用 Cr(Ⅵ) 在土壤中的纵向迁移、静电引力及浓度差渗透实现对土壤 Cr(Ⅵ) 的吸附 (图 4a)。通过测定滤液中 Cr(Ⅵ) 含量, 计算 ATP/PPy 对土壤中 Cr(Ⅵ) 修复效果。由图 4b 可以看出, 当在土壤吸附柱的下方嵌入 ATP/PPy 时, 滤液的颜色明显变浅, 表明原位吸附技术能够显著地降低 Cr(Ⅵ) 在土壤中向下迁移量。

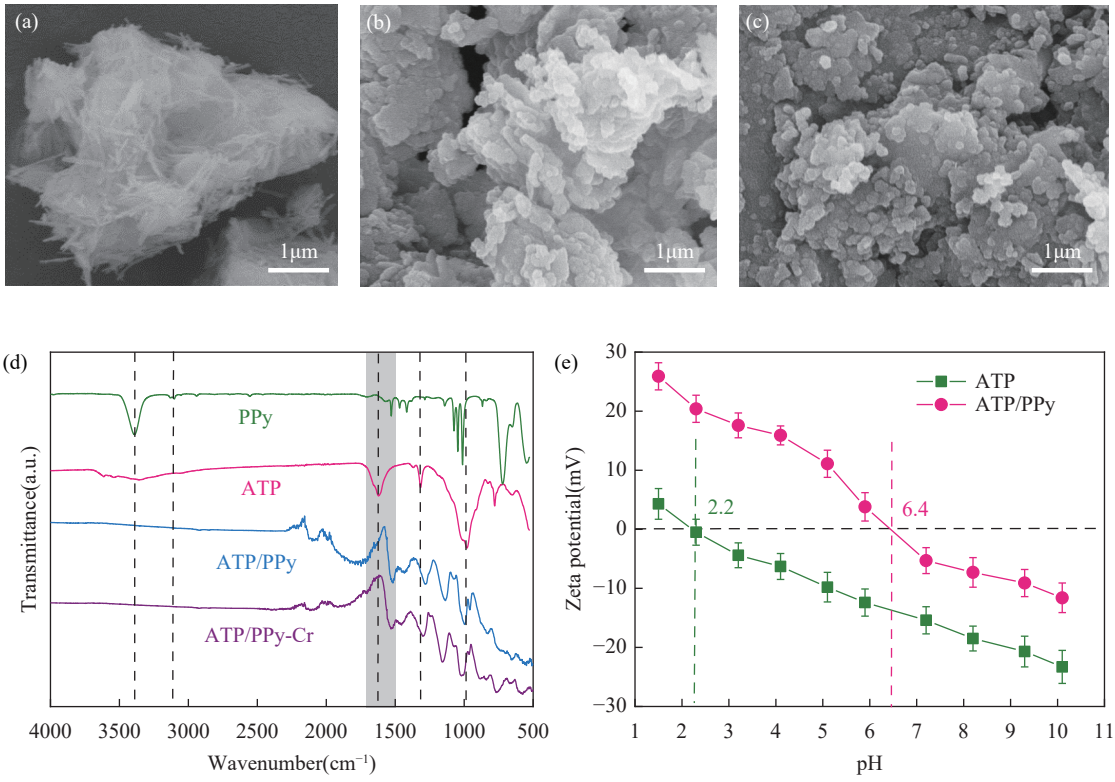

图2　ATP/PPy 吸附材料表征：(a) ATP 的 SEM 图像；(b) ATP/PPy 的 SEM 图像；(c) ATP/PPy 吸附 Cr(Ⅵ) 后 SEM 图像；(d) FTIR 光谱图；(e) Zeta 电位

Fig. 2　Characterization of ATP/PPy adsorbent material: (a) SEM image of ATP; (b) SEM image of ATP/PPy; (c) SEM image of ATP/PPy after Cr(Ⅵ) adsorption; (d) FTIR spectra; (e) Zeta potential.

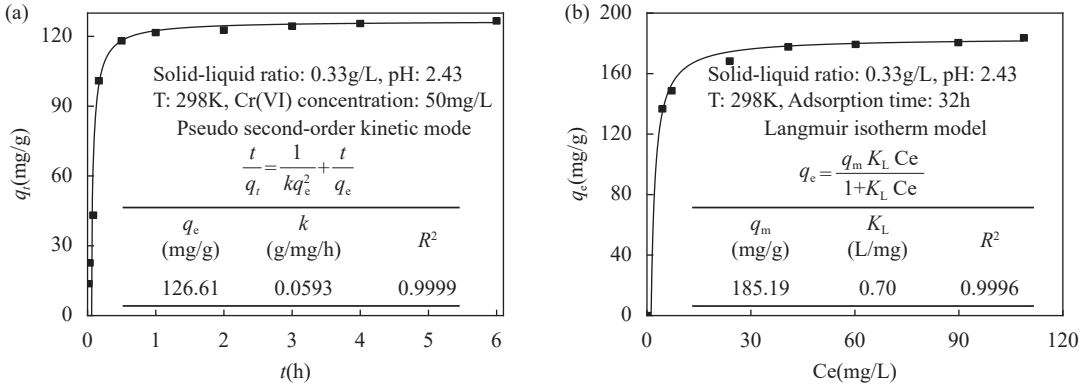

图3　ATP/PPy 对 Cr(Ⅵ) 吸附性能研究：(a) 吸附动力学；(b) 吸附等温线

Fig. 3　The adsorption performance of ATP/PPy for Cr(Ⅵ): (a) Adsorption kinetics; (b) Adsorption isotherms.

2.3.1　降雨量对土壤 Cr(Ⅵ) 修复效果的影响

控制土壤 pH 为 5.86，土壤有机质含量为 7.6g/kg，土壤容重为 1.22g/cm^3，研究模拟降雨量对 ATP/PPy 去除土壤中 Cr(Ⅵ) 效率的影响。实验结果显示，模拟降雨量分别为 38、76、114mm(3、6、9mL/天) 时，对照组 (未添加 ATP/PPy) 滤液中 Cr(Ⅵ) 总含量在第 35 天时趋于稳定，分别为 0.511、0.523、0.534mg。加入 ATP/PPy 后，滤液中 Cr(Ⅵ) 总含量显著降低，且随着降雨量的减少，滤液中 Cr(Ⅵ) 总含量逐渐减少，在第 35 天时滤液中 Cr(Ⅵ) 总含量分别为 0.206、0.217、0.231mg。ATP/PPy 在三种模拟降雨量情况下对滤液中的 Cr(Ⅵ) 去除率分别为 59.69%、58.51%、56.74%，说明原位吸附技术能够显著地降低土壤中 Cr(Ⅵ) 纵向迁移量。另外在第 35 天模拟降雨量分别为 3、6、9mL/天时，ATP/PPy 上层土壤中 Cr(Ⅵ) 的浓度分别降低至 3.37、2.97、2.59mg/kg，均低于《土壤环境质量建设用地土壤污染风险管控标准 (试行)》(GB 36600—2018) 中的建设用地第二类用地筛选值 (5.7mg/kg)。

2.3.2　土壤容重对土壤 Cr(Ⅵ) 修复效果的影响

控制土壤 pH 为 5.86，土壤有机质含量为 7.6g/kg，模拟降雨量为 6mL/天，研究土壤容重对 ATP/PPy 去除土壤中 Cr(Ⅵ) 效率的影响。实验结果显示，在第 35 天土壤容重分别为 1.04、1.22、1.41g/cm^3 时，ATP/PPy 上层土壤中 Cr(Ⅵ) 浓度显著降低，由 30mg/kg 分别降低至 2.75、2.93、3.16mg/kg。另外，当土壤容重分别为 1.04、1.41g/cm^3 时，第 35 天对照组滤液中 Cr(Ⅵ) 总含量分别为 0.534mg、0.516mg(图 4d)。对比添加 ATP/PPy 后，滤液中 Cr(Ⅵ) 总含量分别下降至 0.241mg 与 0.204mg。两种容重下滤液中 Cr(Ⅵ) 的去除率分别为 54.87% 与 60.47%，说明随着土壤容重减少，滤液中 Cr(Ⅵ) 总含量增加。这是由于容重较小的土壤，孔隙率较大，土壤中 Cr(Ⅵ) 迁移速度较快，导致部分 Cr(Ⅵ) 在流经吸附材料时未被吸附。

2.3.3　土壤有机质对土壤 Cr(Ⅵ) 修复效果的影响

控制模拟降雨量为 6mL/天，土壤 pH 为 5.86，土壤容重为 1.22g/cm^3 时，研究土壤有机质含量对 ATP/PPy 去除土壤中 Cr(Ⅵ) 效率的影响。实验结果显示，在第 35 天土壤有机质含量分别为 5.7、7.6、12.4g/kg 时，ATP/PPy 上层土壤中 Cr(Ⅵ) 浓度显著降低，由 30mg/kg 分别降低至 2.85、2.95、3.16mg/kg。同时，第 35 天对照组滤液中 Cr(Ⅵ) 总含量分别为 0.536、0.523 与 0.504mg(图 4e)。添加 ATP/PPy 后，滤液中 Cr(Ⅵ) 总含量分别下降至 0.225、0.217、0.192mg，滤液中 Cr(Ⅵ) 的去除率分别为 58.02%、58.51%、61.90%。随着土壤有机质含量的增加，滤液中 Cr(Ⅵ) 总含量明显减少，这是因为土壤有机质的分解主要是氧化过程，微生物夺取有机质所含的氧，同时形成各种还原物质，与游离的氧及 Cr(Ⅵ) 形成氧化还原系统 [土壤有机质对 Cr(Ⅵ) 的还原解毒作用][32]。同时有机质中富含的含氧官能团，如羟基 (−OH)、羧基 (−COOH)、羰基 (−C=O) 等也可通过螯合吸附部分 Cr(Ⅵ) 离子[33-34]。

2.3.4　土壤 pH 对土壤 Cr(Ⅵ) 修复效果的影响

Cr(Ⅵ) 在环境中的化学形态受 pH 影响较大。在 pH 为 2.0 ~ 6.0 时，Cr(Ⅵ) 主要以 $HCrO_4^-$ 和 $Cr_2O_7^{2-}$ 形式存在；当 pH 高于 6.0 时，主要以 CrO_4^{2-} 形式存在[35]。因此，为了研究 Cr(Ⅵ) 最大去除效率下的最佳 pH 值，控制模拟降雨量为 6mL/天，土壤有机质含量为 7.6g/kg，土壤容重为 1.22g/cm^3，研究不同 pH 土壤对 ATP/PPy 去除 Cr(Ⅵ) 效率的影响。结

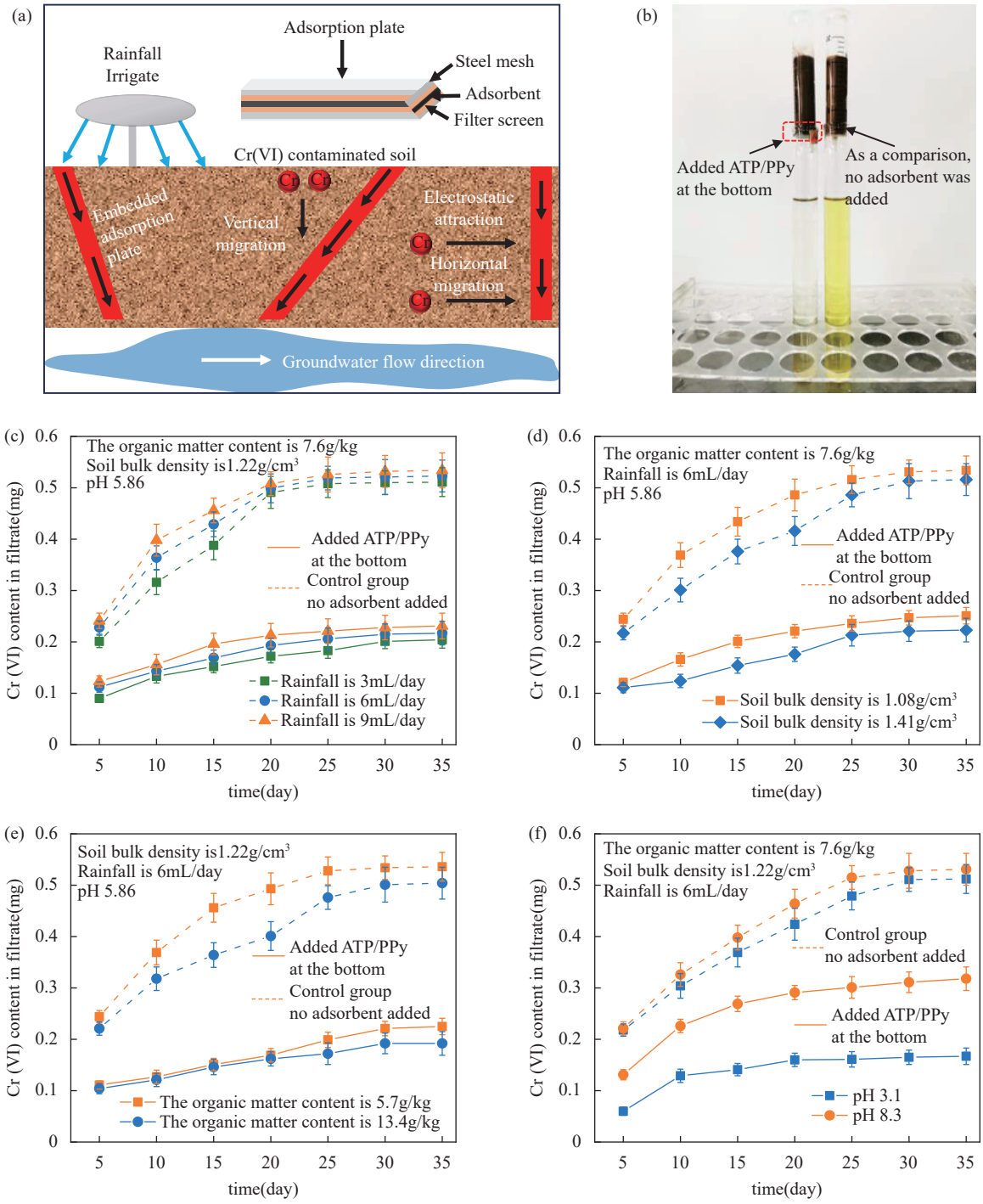

图4　原位吸附技术去除土壤中 Cr(VI) 研究：(a) 原位吸附技术去除土壤中 Cr(VI) 示意图；(b) 模拟降雨量为 76mm(6mL/天) 时，ATP/PPy 对滤液中 Cr(VI) 浓度的影响，左侧柱子为添加 20mg 的 ATP/PPy，右侧柱子为未添加吸附材料；(c) 模拟降雨量对 ATP/PPy 去除滤液中 Cr(VI) 的影响；(d) 土壤容重对 ATP/PPy 去除滤液中 Cr(VI) 的影响；(e) 土壤中有机质含量对 ATP/PPy 去除滤液中 Cr(VI) 的影响；(f) 土壤 pH 对 ATP/PPy 去除滤液中 Cr(VI) 的影响

Fig. 4　*In situ* adsorption technology for removing Cr(VI) from soil: (a) Schematic diagram of *in situ* adsorption technology for removing Cr(VI) from soil; (b) The effect of ATP/PPy on the concentration of Cr(VI) in the filtrate under simulated rainfall of 76mm (6mL/day), with 20mg of ATP/PPy added to the left column and no adsorbent added to the right column; (c) The effect of simulated rainfall on the removal of Cr(VI) from the filtrate by ATP/PPy; (d) The effect of soil bulk density on the removal of Cr(VI) from the filtrate by ATP/PPy; (e) The effect of soil organic matter content on the removal of Cr(VI) from the filtrate by ATP/PPy; (f) The effect of soil pH on the removal of Cr(VI) from the filtrate by ATP/PPy.

果显示, 在第 35 天土壤 pH 值分别为 3.12、5.86 和 8.34 时, ATP/PPy 上层土壤中 Cr(Ⅵ) 浓度显著降低, 由 30mg/kg 分别降低至 2.63、2.97、3.26mg/kg, 同时滤液中 Cr(Ⅵ) 总含量分别为 0.167、0.217 与 0.318mg/kg(图 4f)。对比对照组滤液中 Cr(Ⅵ) 去除率分别为 67.38%、58.51%、40.11%。实验结果说明, 滤液中 Cr(Ⅵ) 去除率受 pH 影响较大, 随着 pH 降低, 滤液中 Cr(Ⅵ) 总含量明显较少。这是由于在较低的 pH 下, ATP/PPy 表面带正电, 可通过静电引力去除大部分 Cr(Ⅵ)。随着 pH 增加, 土壤中氢氧根离子数量增多, 导致其与 CrO_4^{2-}之间存在竞争吸附位点, 使得 Cr(Ⅵ) 去除效率降低[36-37]。

2.4　ATP/PPy 吸附土壤 Cr(Ⅵ) 机理探讨

为了研究 ATP/PPy 对 Cr(Ⅵ) 的吸附机理, 使用 XPS 对 ATP/PPy 吸附 Cr(Ⅵ) 前后进行分析。与 ATP/PPy 相比, 在 ATP/PPy-Cr 中明显观察到 Cr 能带 (图 5a), 说明 ATP/PPy 表面成功加载了 Cr(Ⅵ)。Cr 2p 的核心能级光谱 (图 5b) 显示, Cr(Ⅲ) 和 Cr(Ⅵ) 共存在 ATP/PPy 表面, 说明吸附在 ATP/PPy 表面的部分 Cr(Ⅵ) 被富含电子的 PPy 还原为毒性较小的 Cr(Ⅲ)[38]。Cr 离子和 PPy 之间的反应可用方程式 (1)至(3)进行描述[22]。

$$HCrO_4^- + 3PPy^0 + 7H^+ \rightarrow Cr^{3+} + 4H_2O + 3PPy^+ \quad (1)$$

$$Cr_2O_7^{2-} + 6PPy^0 + 14H^+ \rightarrow 2Cr^{3+} + 7H_2O + 6PPy^+ \quad (2)$$

$$CrO_4^{2-} + 4H_2O + 3PPy^0 \rightarrow Cr^{3+} + 8OH^- + 3PPy^+ \quad (3)$$

式中: PPy^0 和 PPy^+代表聚吡咯的还原态和氧化态。

N 1s 核心能级光谱 (图 5c) 显示, 与 ATP/PPy 相比, ATP/PPy-Cr 中=NH−和−NH−基团的峰面积比降低, 但$-NH^+-$基团的百分比增加, 表明 PPy 表面 N 基团通过静电引力和还原参与了对 Cr(Ⅵ) 的吸附。同时去质子化的吡咯 N 可与 Cr(Ⅲ) 形成配合物, 通过 Cr(Ⅲ)-N 共价键吸附 Cr(Ⅲ)[22]。此外, ATP/PPy 吸附 Cr(Ⅵ) 后, Cl 的峰面积显著减小 (图 5d), 这证明 ATP/PPy 中掺杂的 Cl^-和 Cr(Ⅵ) 之间发生离子交换[39-41]。基于上述分析, 得出 ATP/PPy 吸附 Cr(Ⅵ) 的 4 种机制 (图 1): ① ATP/PPy 中带正

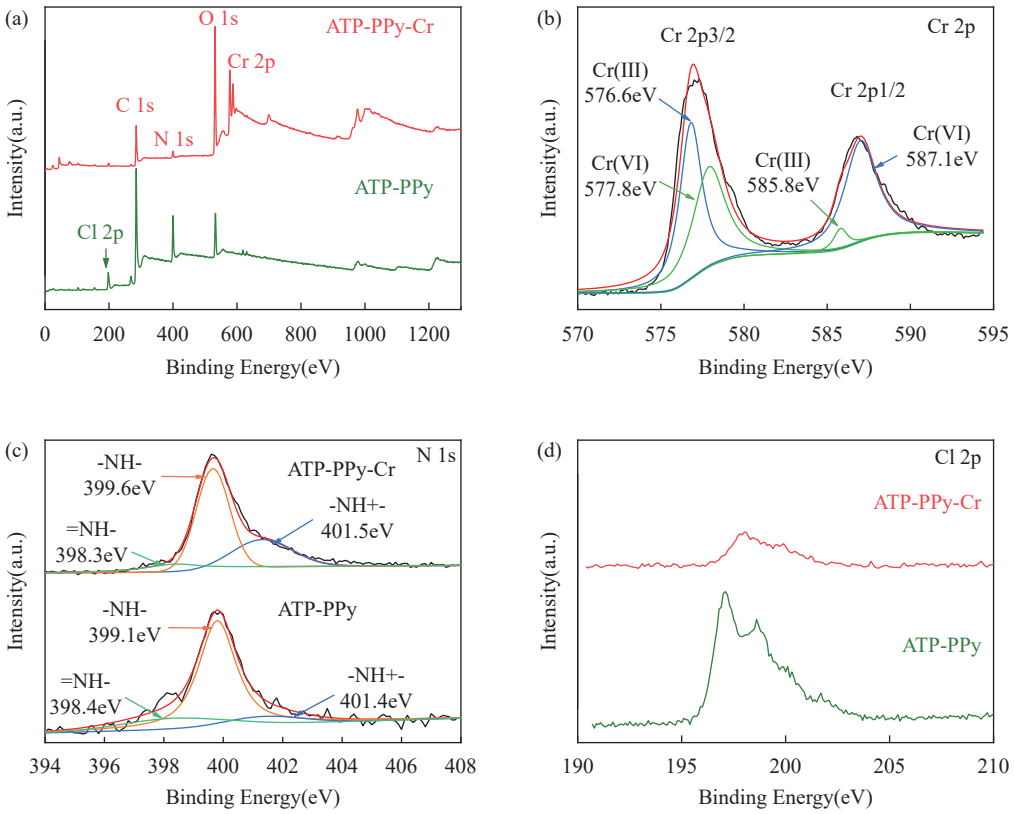

图5　XPS 光谱分析: (a) ATP/PPy **吸附** Cr(Ⅵ) **前后的宽扫描** XPS **光谱;** (b) Cr 2p **光谱;** (c) N 1s **谱;** (d) Cl 2p **光谱**

Fig. 5　XPS spectral analysis: (a) Wide-scan XPS spectra of ATP/PPy before and after Cr(Ⅵ) adsorption; (b) Cr 2p spectra; (c) N 1s spectra; (d) Cl 2p spectra.

电的 N 通过静电引力去除 Cr(Ⅵ); ② Cr(Ⅵ) 在 PPy 氮基团的作用下被还原成 Cr(Ⅲ); ③ Cr(Ⅲ) 被螯合在去质子化的吡咯 N 上; ④ Cr(Ⅵ) 通过离子交换取代掺杂在 ATP/PPy 中的 Cl^-。

3　结论

将 PPy 以原位聚合的方式负载在 ATP 表面, 制备了以 PPy 为“壳”和以 ATP 为“核”的 ATP/PPy 吸附材料。ATP/PPy 对 Cr(Ⅵ) 具有较高吸附亲和力和吸附特异性。吸附动力学研究表明, ATP/PPy 对 Cr(Ⅵ) 的吸附遵循伪二级动力学模型, 说明吸附过程主要是化学吸附, 且在 30min 内能够达到 95% 的平衡吸附量。吸附等温线研究表明, ATP/PPy 对 Cr(Ⅵ) 的吸附遵循 Langmuir 等温吸附模型, 说明 ATP/PPy 对 Cr(Ⅵ) 的吸附过程是单层吸附, 最大吸附量为 185.19mg/g。吸附机理包括静电引力、螯合、还原与离子交换。

将 ATP/PPy 嵌入土壤中, 通过原位吸附的方式修复 Cr(Ⅵ) 污染土壤。结果表明, 当供试土壤中 Cr(Ⅵ) 浓度为 30mg/kg, 模拟降雨量为 6mL/天, 土壤有机质含量为 7.6g/kg, 土壤容重为 1.22g/cm^3, 土壤 pH 为 5.86, 第 35 天时土壤滤液中 Cr(Ⅵ) 去除率为 58.51%, 土壤中 Cr(Ⅵ) 的含量降至 2.97mg/kg, 低于《土壤环境质量建设用地土壤污染风险管控标准(试行)》(GB 36600—2018) 中的建设用地第二类用地筛选值 5.7mg/kg。另外, 实际 Cr(Ⅵ) 污染土壤中成分较为复杂, 目前该研究考察因素较少, 参考土壤类型较为单一, 在后续 Cr(Ⅵ) 污染场地修复中还需要进一步研究其影响因素。总体而言, 对比常见的 Cr(Ⅵ) 污染场地修复技术如客土法、还原法、固化法、生物法等, 该技术具有实施工期短、对周边环境扰动小、修复成本低等优势, 有望在实际应用中高效低成本地修复 Cr(Ⅵ) 污染场地。

In situ Adsorption Technology for Remediation of Cr(Ⅵ) Contaminated Soil

ZHANG Zhaoxin[1,2,3], *CAO Ningning*[1], *LI Linji*[1,2], *LIU Suqing*[1], *LI Jiahao*[1], *CAO Cui*[1], *LI Heping*[1], *ZHANG Kai*[1], *SHI Yongli*[1,2,3*]

(1. Geological Experiment and Testing Institute, Henan Academy of Geology, Zhengzhou 450018, China;
2. Key Laboratory of Water and Soil Resources Protection and Rehabilitation in the Middle and Lower Reaches of the Yellow River Basin, Ministry of Natural Resources, Zhengzhou 450052, China;
3. Henan Province Natural Resources Science and Technology Innovation Center (Research on Water and Soil Ecological Restoration and Management), Zhengzhou 450052, China)

HIGHLIGHTS

(1) ATP/PPy composite materials with strong adsorption affinity for Cr(Ⅵ) were prepared. ATP/PPy can effectively remove Cr(Ⅵ) from aqueous solutions and soil. The adsorption mechanisms include electrostatic attraction, chelation, reduction, and ion exchange.

(2) The adsorption of Cr(Ⅵ) by ATP/PPy follows the pseudo-second-order kinetic model, indicating that the adsorption process is mainly chemical adsorption. The adsorption of Cr(Ⅵ) by ATP/PPy follows the Langmuir isotherm model, indicating that the removal process of Cr(Ⅵ) by ATP/PPy is monolayer adsorption, with a maximum adsorption capacity of 185.19mg/g.

(3) The remediation experimental results of ATP/PPy on Cr(Ⅵ) contaminated soil under different conditions through *in situ* adsorption technology show that after 30 days of remediation under optimal conditions, Cr(Ⅵ) in the soil filtrate decreased by 58.51%, and the Cr(Ⅵ) content in the soil decreased to 2.97mg/kg.

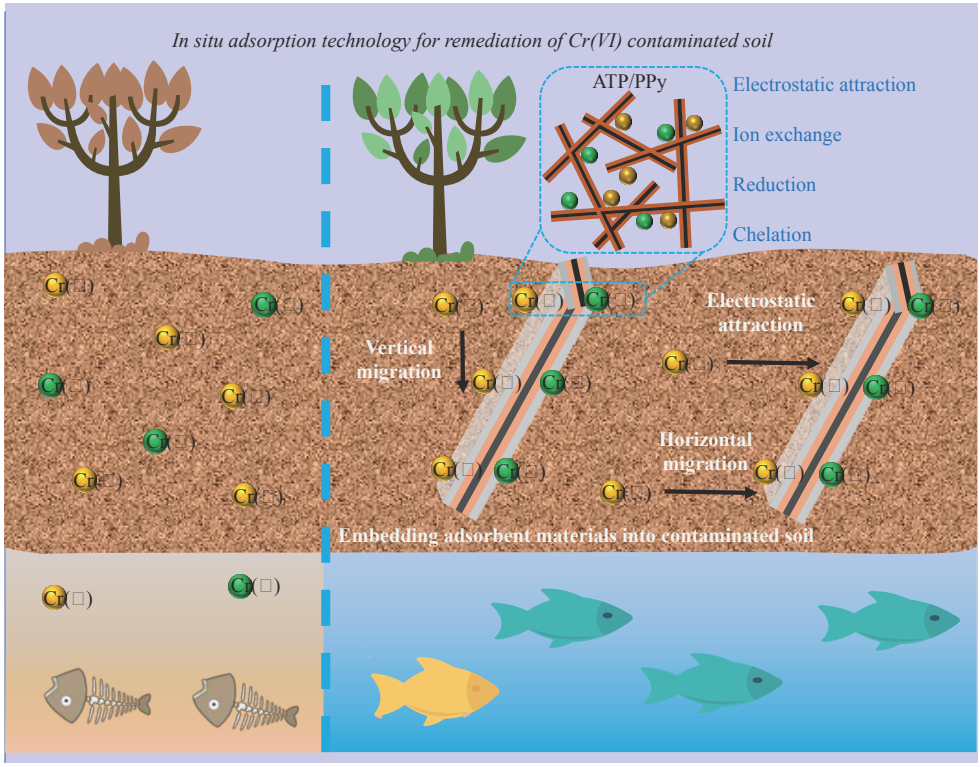

ABSTRACT: The commonly used remediation technologies for Cr(Ⅵ) contaminated soil, such as guest soil, reduction, solidification, microbiology, etc., have drawbacks such as high cost, slow efficiency, and secondary oxidation of Cr(Ⅵ). To solve these problems, a Cr(Ⅵ) contaminated soil remediation technology was developed. Firstly, polypyrrole was loaded onto the surface of attapulgite through *in situ* polymerization to prepare ATP/PPy adsorption material with PPy as the "shell" and ATP as the "core". Then, ATP/PPy was embedded into the soil and remediate Cr(Ⅵ) contaminated soil through *in situ* adsorption technology. The experimental results show that under optimal conditions, the removal rate of Cr(Ⅵ) in soil filtrate was 58.51%, and the Cr(Ⅵ) content in the soil was reduced to 2.97mg/kg, which was lowered to below the screening value of 5.7mg/kg for the second category of development land in the *Soil Environmental Quality: Risk Control Standard for Soil Contamination of Development Land* (GB 36600—2018). Meanwhile, this technology has the advantages of simple operation, economic and environmental protection, high remediation efficiency, and thorough removal, and can be used for the remediation and treatment of actual Cr(Ⅵ) contaminated soil. The BRIEF REPORT is available for this paper at http://www.ykcs.ac.cn/en/article/doi/10.15898/j.ykcs.202307090090.

KEY WORDS: attapulgite; polypyrrole; soil remediation; hexavalent chromium; *in situ* adsorption

BRIEF REPORT

Significance: Cr is widely used in industrial and agricultural activities, such as leather tanning, metallurgy, electroplating, ceramic glaze, and wood anti-corrosion. It is listed by the international community as one of the eight most competitive resource-based raw material products[1-3]. However, with the development of industry, a large amount of Cr enters the environment along with the discharge of wastewater and waste residue, leaving behind a large number of Cr pollution sites[4-6]. The main forms of Cr in soil are Cr(Ⅲ) and Cr(Ⅵ). Due to the negative charge of the soil, Cr(Ⅲ) is easily adsorbed or precipitated by soil colloids, with low activity and less toxicity to organisms. However, Cr(Ⅵ) has weak adsorption and strong migration with soil colloids, making it easy to

accumulate and enter the human body through the food chain. After Cr(Ⅵ) enters the human body, its anionic compound (CrO_4^{2-}) has a chemical structure similar to SO_4^{2-} and HPO_4^{2-} in the intracellular fluid. It can easily enter the cell through protein channels on the cell membrane, react with reducing substances such as ascorbic acid, and damage the DNA in the nucleus, causing diseases such as lung cancer, birth defects, and decreased reproductive ability[7]. Due to the enormous harm of Cr(Ⅵ), Cr(Ⅵ) and its compounds are listed as one of the 17 highly hazardous toxic substances by the US Environmental Protection Agency (EPA)[8-10]. Therefore, research on the remediation and treatment of Cr(Ⅵ) contaminated sites has received widespread attention from environmental workers in various countries.

According to reports, 11% of contaminated sites in the United States, and 14% of contaminated sites in Japan are Cr(Ⅵ) contaminated[11]. The area of Cr contaminated soil in China accounts for more than 5% of the total polluted soil area[12]. In recent years, researchers have developed various *in situ* and *ex situ* remediation technologies to accommodate, clean, or restore Cr contaminated soil, such as guest soil method, soil washing, electric extraction, chemical reduction, and phytoremediation[13-16]. These remediation methods have different working mechanisms and demonstrate specific application advantages and limitations. In addition, due to differences in physical and chemical soil properties, texture, pollution situation, etc., the effectiveness and cost of these technologies in on site practice vary greatly. For example, the cost of guest soil method and soil washing technology is extremely high, and they cause significant disturbance to the surrounding environment. They are only suitable for small-scale, high concentration Cr(Ⅵ) polluted sites; chemical reduction is currently a common method for remediation of Cr(Ⅵ) contaminated sites, but the reduced Cr(Ⅲ) poses a risk of being re-oxidized to Cr(Ⅵ); the electric extraction method has high energy consumption and the actual site restoration effect is not ideal; the efficiency of plant restoration is low and the cycle is long. Therefore, based on the concept of green and sustainable development, developing a new technology, method, and material for economically efficient and environmentally friendly remediation of Cr(Ⅵ) contaminated sites is a key issue that urgently needs to be addressed.

Methods: ATP/PPy adsorbent materials were prepared with PPy as the "shell" and ATP as the "core" by loading polypyrrole onto the surface of attapulgite through *in situ* polymerization (Fig.1). ATP/PPy has high adsorption affinity and specificity for Cr(Ⅵ), and can remove Cr(Ⅵ) through electrostatic attraction, chelation, reduction, and ion exchange. Meanwhile, ATP/PPy is embedded into the soil through adsorption plates, relying on the vertical migration and concentration difference infiltration of Cr(Ⅵ) in the soil to achieve *in situ* adsorption of Cr(Ⅵ) in the soil, and complete the recovery and regeneration of ATP/PPy after adsorption saturation. The effects of four factors, namely rainfall, soil pH, soil bulk density, and soil organic matter content, on the removal of Cr(Ⅵ) from soil by ATP/PPy were investigated to understand the feasibility of adsorption technology for the remediation of Cr(Ⅵ) contaminated soil.

Data and Results: Scanning electron microscopy analysis shows that the unmodified ATP was a blocky structure formed by rod crystal stacking (Fig.2a), and ATP/PPy was coated with PPy microspheres on the surface of ATP (Fig.2b). At the same time, after adsorption of Cr(Ⅵ), the surface morphology of ATP/PPy remained almost unchanged (Fig.2c). The FTIR specta (Fig.2d) show that the characteristic peaks of ATP at 3560cm^{-1} and 3419cm^{-1} correspond to the −OH stretching vibration caused by mineral layer and surface adsorbed water, while the peak at 1665cm^{-1} corresponds to the −OH stretching vibration of H_2O. In addition, the peaks at 1037cm^{-1} and 791cm^{-1} are attributed to Si−O−Si stretching vibration and bending vibration, respectively. The characteristic peak of PPy at 1555cm^{-1} corresponds to the C−C stretching vibration of the pyrrole ring, the characteristic peak at 1160cm^{-1} corresponds to the C−N stretching vibration, and the characteristic peaks at 1030cm^{-1} and 772cm^{-1} correspond to the in-plane stretching vibration peak and the out of plane bending vibration peak of the C−H ring, respectively. The FTIR spectrum of ATP/PPy clearly showed the characteristic absorption peak of PPy, indicating that PPy has been

successfully loaded onto the surface of ATP[25-26]. In addition, after adsorbing Cr(Ⅵ), the infrared spectra of ATP/PPy-Cr shift towards higher values, such as 1565cm^{-1}, 1390cm^{-1}, 1210cm^{-1}, 1045cm^{-1}, and 912cm^{-1}. This is due to the presence of different forms of Cr in ATP/PPy, which leads to the destruction of the conjugated structure of PPy and the limitation of the degree of charge delocalization in PPy[22]. The zero potential display shows that due to the introduction of PPy, the zero potential of ATP/PPy increases from 2.2 to 6.4 (Fig.2e), which is beneficial for ATP/PPy to remove negatively charged Cr(Ⅵ) through electrostatic attraction[27].

The adsorption kinetics of ATP/PPy for Cr(Ⅵ) in water were shown in Fig.3a. The experimental data shows that ATP/PPy had a fast adsorption rate for Cr(Ⅵ), reaching an equilibrium adsorption capacity of 95% within 30min. In addition, the pseudo-second-order kinetic model perfectly fitted the adsorption data of ATP/PPy for Cr(Ⅵ), with a correlation coefficient R^2>0.9999, indicating that the adsorption process was mainly chemical adsorption[28-29]. In order to explore the maximum adsorption capacity of ATP/PPy for Cr(Ⅵ), adsorption isotherms were studied (Fig.3b). The results show that the adsorption capacity of ATP/PPy for Cr(Ⅵ) increased with the initial concentration of Cr(Ⅵ). The Langmuir model can better fit the adsorption data of ATP/PPy for Cr(Ⅵ), with a correlation coefficient R^2>0.9996, revealing that the removal process of Cr(Ⅵ) by ATP/PPy was monolayer adsorption[30-31]. At 25℃, the maximum adsorption capacity of ATP/PPy for Cr(Ⅵ) was 185.19mg/g, indicating that ATP/PPy had strong removal ability for Cr(Ⅵ).

In order to study the removal mechanism of Cr(Ⅵ) by ATP/PPy, XPS was used to analyze the adsorption of Cr(Ⅵ) by ATP/PPy before and after. Compared with ATP/PPy, Cr energy bands were clearly observed in ATP/PPy-Cr (Fig.4a), indicating the successful loading of Cr on the surface of ATP/PPy. The core energy level spectrum of Cr 2p shows that Cr(Ⅲ) and Cr(Ⅵ) coexist on the surface of ATP/PPy (Fig.4b), indicating that the portion of Cr(Ⅵ) adsorbed on the surface of ATP/PPy was reduced to less toxic Cr(Ⅲ) by electron rich PPy[38]. The core energy level spectrum of N 1s shows that compared with ATP/PPy, the peak area ratio of NH− and −NH− groups in ATP/PPy-Cr decreased (Fig.4c), but the percentage of $-NH^+$-groups increased, indicating that the N groups on the PPy surface participate in the adsorption of Cr(Ⅵ) through adsorption and reduction[22]. In addition, after the adsorption of Cr(Ⅵ) by ATP/PPy, the peak area of Cl 2p significantly decreased (Fig.4d), indicating ion exchange between Cl^- doped in ATP/PPy and Cr(Ⅵ)[39-41]. Based on XPS analysis, four mechanisms for removing Cr(Ⅵ) by ATP/Ppy were identified (Fig.1): (1) The positively charged N in ATP/PPy removes Cr(Ⅵ) through electrostatic attraction; (2) Cr(Ⅵ) is reduced to Cr(Ⅲ) by the action of nitrogen groups in PPy; (3) Cr(Ⅲ) is chelated onto deprotonated pyrrole N; (4) Cr(Ⅵ) replaces Cl^- doped in ATP/PPy through ion exchange.

ATP/PPy was embedded into the soil through adsorption plates and Cr(Ⅵ) was removed from the soil through *in situ* adsorption technology (Fig.5a). We investigated the effects of different factors namely rainfall, soil pH, soil bulk density, and soil organic matter content on the removal efficiency of Cr(Ⅵ) in soil. The experimental results show that when the concentration of Cr(Ⅵ) in the tested soil was 30mg/kg, the simulated rainfall was 6mL/day, the soil bulk organic matter content was 7.6g/kg, the soil bulk density was 1.22g/cm^3, and the soil pH was 5.86, the removal rate of Cr(Ⅵ) in the soil filtrate was 58.51% (Fig.5b). The Cr(Ⅵ) content in the soil decreased to 2.97mg/kg (Fig.5c, Fig.5d, Fig.5e, Fig.5f), which was lowered to below the screening value of 5.7mg/kg for the second category of development land in the *Soil Environmental Quality: Risk Control Standard for Soil Contamination of Development Land* (GB 36600—2018).

参考文献

[1] 褚琳琳, 王静云, 金晓霞, 等. 碱溶液提取-离子交换-电感耦合等离子体质谱法测定土壤中六价铬[J]. 岩矿测试, 2022, 41(5): 826−835.
Chu L L, Wang J Y, Jin X X, et al. Determination of hexavalent chromium in soil by inductively coupled plasma-mass spectrometry with alkaline digestion-ion exchange[J]. Rock and Mineral Analysis, 2022, 41(5): 826−835.

[2] Ertani A, Mietto A, Borin M, et al. Chromium in agricultural soils and crops: A review[J]. Water, Air, & Soil Pollution, 2017, 228: 1-12.

[3] Hausladen D M, Alexander-Ozinskas A, McClain C, et al. Hexavalent chromium sources and distribution in California groundwater[J]. Environmental Science & Technology, 2018, 52(15): 8242−8251.

[4] Coetzee J J, Bansal N, Chirwa E M N. Chromium in environment, its toxic effect from chromite-mining and ferrochrome industries, and its possible bioremediation[J]. Exposure and Health, 2020, 12: 51−62.

[5] 石勇丽, 夏辉, 曹宁宁, 等. 碱液提取-树脂除盐结合电感耦合等离子体发射光谱法测定土壤中 Cr(Ⅵ)[J]. 分析科学学报, 2021, 37(6): 771−776.
Shi Y L, Xia H, Cao N N, et al. Determination of Cr(Ⅵ) in soil by lye extraction-resin desalination combined with ICP-OES[J]. Journal of Analytical Science, 2021, 37(6): 771−776.

[6] Kerur S S, Bandekar S, Hanagadakar M S, et al. Removal of hexavalent chromium-industry treated water and wastewater: A review[J]. Materials Today: Proceedings, 2021, 42: 1112−1121.

[7] Monga A, Fulke A B, Dasgupta D. Recent developments in essentiality of trivalent chromium and toxicity of hexavalent chromium: Implications on human health and remediation strategies[J]. Journal of Hazardous Materials Advances, 2022, 7: 100113.

[8] Sharma P, Singh S P, Parakh S K, et al. Health hazards of hexavalent chromium [Cr(Ⅵ)] and its microbial reduction[J]. Bioengineered, 2022, 13(3): 4923−4938.

[9] Marinho B A, Cristóvão R O, Boaventura R A R, et al. As(Ⅲ) and Cr(Ⅵ) oxyanion removal from water by advanced oxidation/reduction processes—A review[J]. Environmental Science and Pollution Research, 2019, 26: 2203−2227.

[10] 邓日欣, 罗伟嘉, 韩奕彤, 等. 膨润土负载纳米铁镍同步修复地下水中三氯乙烯和六价铬复合污染[J]. 岩矿测试, 2018, 37(5): 541−548.
Deng R X, Luo W J, Han Y T, et al. Simultaneous removal of TCE and Cr(Ⅵ) in groundwater by using bentonite-supported nanoscale Fe/Ni[J]. Rock and Mineral Analysis, 2018, 37(5): 541−548.

[11] Suzuki T, Kawai K, Moribe M, et al. Recovery of Cr as Cr(Ⅲ) from Cr(Ⅵ)-contaminated kaolinite clay by electrokinetics coupled with a permeable reactive barrier[J]. Journal of Hazardous Materials, 2014, 278: 297−303.

[12] Xia S, Song Z, Jeyakumar P, et al. Characteristics and applications of biochar for remediating Cr(Ⅵ)-contaminated soils and wastewater[J]. Environmental Geochemistry and Health, 2020, 42: 1543−1567.

[13] 杨文晓, 张丽, 毕学, 等. 六价铬污染场地土壤稳定化修复材料研究进展[J]. 环境工程, 2020, 38(6): 16−23.
Yang W X, Zhang L, Bi X, et al. Research advancement of stabilization materials for hexavalent chromium(Ⅵ) contaminated site soils[J]. Environmental Engineering, 2020, 38(6): 16−23.

[14] 刘益风, 李洁, 申源源, 等. 重庆某六价铬污染场地土壤修复工程案例[J]. 广州化工, 2019, 47(12): 111−114.
Liu Y F, Li J, Shen Y Y, et al. Soil remediation engineering instances of a hexavalent chromium contaminated site in Chongqing[J]. Guangzhou Chemical Industry, 2019, 47(12): 111−114.

[15] 安茂国, 赵庆令, 谭现锋, 等. 化学还原-稳定化联合修复铬污染场地土壤的效果研究[J]. 岩矿测试, 2019, 38(2): 204−211
An M G, Zhao Q L, Tan X F, et al. Research on the effect of chemical reduction-stabilization combined remediation of contaminated soil[J]. Rock and Mineral Analysis, 2019, 38(2): 204−211.

[16] 曹宁宁, 李林记, 石勇丽, 等. 土壤六价铬污染修复技术研究进展与应用探讨[J]. 磷肥与复肥, 2023, 38(4): 42−48.
Cao N N, Li L J, Shi Y L, et al. Research progress and application discussion on remediation technology of Cr(Ⅵ) contaminated soil[J]. Phosphate & Compound Fertilize, 2023, 38(4): 42−48.

[17] Liu L, Li X, Wang X, et al. Metolachlor adsorption using walnut shell biochar modified by soil minerals[J]. Environmental Pollution, 2022, 308: 119610.

[18] Qiu M, Liu L, Ling Q, et al. Biochar for the removal of contaminants from soil and water: A review[J]. Biochar, 2022, 4(1): 19.

[19] Li A, Ge W, Liu L, et al. Synthesis and application of amine-functionalized $MgFe_2O_4$-biochar for the adsorption and immobilization of Cd(Ⅱ) and Pb(Ⅱ)[J]. Chemical Engineering Journal, 2022, 439: 135785.

[20] Li Y, Gao Y, Zhang Q, et al. Flexible and free-standing pristine polypyrrole membranes with a nanotube structure for repeatable Cr(Ⅵ) ion removal[J]. Separation and Purification Technology, 2021, 258:

117981.

[21] Mahmud H N M E, Huq A K O, Yahya R B. The removal of heavy metal ions from wastewater/aqueous solution using polypyrrole-based adsorbents: A review[J]. RSC Advances, 2016, 6(18): 14778−14791.

[22] Xiang L, Niu C G, Tang N, et al. Polypyrrole coated molybdenum disulfide composites as adsorbent for enhanced removal of Cr(Ⅵ) in aqueous solutions by adsorption combined with reduction[J]. Chemical Engineering Journal, 2021, 408: 127281.

[23] 张凯. 凹凸棒土棒晶束解离研究[D]. 郑州: 郑州大学, 2019.
Zhang K. Researches of crystal-bundles dissociation of palygorskite[D]. Zhengzhou: Zhengzhou University, 2019.

[24] 化全县, 郝志远, 张凯, 等. 水热酸处理解离凹凸棒土晶束的研究[J]. 应用化工, 2020, 49(8): 1904−1908.
Hua Q X, Hao Z Y, Zhang K, et al. Study on attapulgite crystal bundles dissociation by hydrothermal acid technology[J]. Applied Chemical Industry, 2020, 49(8): 1904−1908.

[25] 陈泳. 具有选择吸附作用的聚吡咯/凹凸棒复合材料吸附性能[D]. 兰州: 兰州理工大学, 2018.
Chen Y. The adsorption properties of polypyrrole/attapulgite composites with selective adsorption[D]. Lanzhou: Lanzhou University of Technology, 2018.

[26] Wang L, Muhammad H, Laipan M, et al. Enhanced removal of Cr(Ⅵ) and Mo(Ⅵ) from polluted water using L-cysteine doped polypyrrole/bentonite composite[J]. Applied Clay Science, 2022, 217: 106387.

[27] Yu H, Chen H, Zhang P, et al. *In situ* self-sacrificial synthesis of polypyrrole/biochar composites for efficiently removing short- and long-chain perfluoroalkyl acid from contaminated water[J]. Journal of Environmental Management, 2023, 344: 118745.

[28] Chen S, Yue Q, Gao B, et al. Equilibrium and kinetic adsorption study of the adsorptive removal of Cr(Ⅵ) using modified wheat residue[J]. Journal of Colloid and Interface Science, 2010, 349(1): 256−264.

[29] Zhang K, Dai Z, Zhang W, et al. EDTA-based adsorbents for the removal of metal ions in wastewater[J]. Coordination Chemistry Reviews, 2021, 434: 213809.

[30] Zhao S, Li Z, Wang H, et al. Effective removal and expedient recovery of As(Ⅴ) and Cr(Ⅵ) from soil by layered double hydroxides coated waste textile[J]. Separation and Purification Technology, 2021, 263: 118419.

[31] Yang D, Wang L, Li Y, et al. Pseudocapacitive deionization of high concentrations of hexavalent chromium using NiFe-layered double hydroxide/polypyrrole asymmetric electrode[J]. Separation and Purification Technology, 2024, 328: 125004.

[32] Ren Z, Xu X, Wang X, et al. FTIR, Raman, and XPS analysis during phosphate, nitrate and Cr(Ⅵ) removal by amine cross-linking biosorbent[J]. Journal of Colloid and Interface Science, 2016, 468: 313−323.

[33] Deng L, Liu F, Ding Z, et al. Effect of natural organic matter on Cr(Ⅵ) reduction by reduced nontronite[J]. Chemical Geology, 2023, 615: 121198.

[34] Ambika S, Kumar M, Pisharody L, et al. Modified biochar as a green adsorbent for removal of hexavalent chromium from various environmental matrices: Mechanisms, methods, and prospects[J]. Chemical Engineering Journal, 2022, 439: 135716.

[35] Zhang Y, Liu J, Wu X, et al. Ultrasensitive detection of Cr(Ⅵ)($Cr_2O_7^{2-}$/CrO_4^{2-}) ions in water environment with a fluorescent sensor based on metal-organic frameworks combined with sulfur quantum dots[J]. Analytica Chimica Acta, 2020, 1131: 68−79.

[36] Xu Y, Chen J, Chen R, et al. Adsorption and reduction of chromium(Ⅵ) from aqueous solution using polypyrrole/calcium rectorite composite adsorbent[J]. Water Research, 2019, 160: 148−157.

[37] Ko Y J, Choi K, Lee S, et al. Strong chromate-adsorbent based on pyrrolic nitrogen structure: An experimental and theoretical study on the adsorption mechanism[J]. Water Research, 2018, 145: 287−296.

[38] Qiu L, Wang Y, Sui R, et al. Preparation of a novel metal-free polypyrrole-red phosphorus adsorbent for efficient removal of Cr(Ⅵ) from aqueous solution[J]. Environmental Research, 2023, 224: 115458.

[39] Zhou F, Li Y, Wang S, et al. Turning waste into valuables: *In situ* deposition of polypyrrole on the obsolete mask for Cr(Ⅵ) removal and desalination[J]. Separation and Purification Technology, 2023, 306: 122643.

[40] Xing J, Zhu C, Chowdhury I, et al. Electrically switched ion exchange based on polypyrrole and carbon nanotube nanocomposite for the removal of chromium(Ⅵ) from aqueous solution[J]. Industrial & Engineering Chemistry Research, 2018, 57(2): 768−774.

[41] Shi Y, Feng J, Zhang Z, et al. Simultaneous removal of Cr(Ⅵ) anions and metal cations by EDTA-crosslinking-chitosan/polypyrrole composites[J]. Separation and Purification Technology, 2023, 327: 124926.